REPORT DOCUMENTATION PAGE

1a. REPORT SECURITY CLASSIFICATION Unclassified	1b. RESTRICTIVE MARKINGS None
2a. SECURITY CLASSIFICATION AUTHORITY N/A	3. DISTRIBUTION/AVAILABILITY OF REPORT Approved for public release; distribution unlimited.
2b. DECLASSIFICATION/DOWNGRADING SCHEDULE N/A	
4. PERFORMING ORGANIZATION REPORT NUMBER(S) NRL Memorandum Report 5616	5. MONITORING ORGANIZATION REPORT NUMBER(S) N/A
6a. NAME OF PERFORMING ORGANIZATION Underwater Sound Ref. Detach. Naval Research Laboratory 6b. OFFICE SYMBOL (If applicable) 5970	7a. NAME OF MONITORING ORGANIZATION N/A
6c. ADDRESS (City, State, and ZIP Code) P.O. Box 8337 Orlando, FL 32856-8337	7b. ADDRESS (City, State, and ZIP Code) N/A
8a. NAME OF FUNDING/SPONSORING ORGANIZATION Naval Oceanographic Office 8b. OFFICE SYMBOL (If applicable) None	9. PROCUREMENT INSTRUMENT IDENTIFICATION NUMBER Lost
8c. ADDRESS (City, State, and ZIP Code) Bay St. Louis NSTL, MS 39522	10. SOURCE OF FUNDING NUMBERS PROGRAM ELEMENT NO.: 0&MN PROJECT NO.: None TASK NO.: None WORK UNIT ACCESSION NO.: (59)S600-0

11. TITLE (Include Security Classification)
A TRANSDUCER FOR BOTTOM-SCATTERING MEASUREMENTS

12. PERSONAL AUTHOR(S)
A. C. Tims, T. A. Henriquez, and J. G. Williams

13a. TYPE OF REPORT	13b. TIME COVERED	14. DATE OF REPORT (Year, Month, Day)	15. PAGE COUNT
Final	FROM Jan 81 TO Jan 82	31 December 1985	25

16. SUPPLEMENTARY NOTATION
None

17. COSATI CODES			18. SUBJECT TERMS (Continue on reverse if necessary and identify by block number)
FIELD	GROUP	SUB-GROUP	Transducer; hydrophone, omnidirectional, preamplifier, bottom scattering, modeling & analysis
20	01		
17	01		

19. ABSTRACT (Continue on reverse if necessary and identify by block number)

An omnidirectional 25-kHz transducer has been designed for use in bottom-scattering measurements. The transducer can be used either as a projector or when fitted with a preamplifier, as a hydrophone. The requirements for the design are presented and solved with mathematical modeling and analysis. A comparison between theory and measured performance is given. The design of a low-noise preamplifier with integrated circuits is described.

20. DISTRIBUTION/AVAILABILITY OF ABSTRACT ☒ UNCLASSIFIED/UNLIMITED ☐ SAME AS RPT. ☐ DTIC USERS	21. ABSTRACT SECURITY CLASSIFICATION Unclassified
22a. NAME OF RESPONSIBLE INDIVIDUAL Allan C. Tims	22b. TELEPHONE (Include Area Code) 305, 857-5115 22c. OFFICE SYMBOL 5977

DD FORM 1473, 84 MAR 83 APR edition may be used until exhausted. All other editions are obsolete.

NRL-Memorandum Report-5616

A TRANSDUCER FOR BOTTOM-SCATTERING MEASUREMENTS

A.C. Tims, T.A. Henriquez, and J.G. Williams

Underwater Sound Reference Detachment
P.O. Box 568337
Orlando, Florida 32856-8337

31 December 1985

NAVAL RESEARCH LABORATORY
Washington, D.C.

CONTENTS

A TRANSDUCER FOR BOTTOM-SCATTERING MEASUREMENTS

INTRODUCTION

Part of the mission of the U.S. Naval Oceanographic Office (NAVOCEANO) is to support the U.S. Navy by collecting ocean acoustic data from all parts of the world. Ocean-bottom acoustic scattering and volume reverberation data are very important to the Navy's Antisubmarine Warfare program and as such have a high priority in NAVOCEANO'S mission. The instrumentation used in the past to gather this data has been made up from parts of other systems and was not optimized for the measurement. To upgrade the quality and reliability of measurements, the Underwater Sound Reference Detachment (USRD) of the Naval Research Laboratory worked with NAVOCEANO in a cooperative effort to develop an optimized set of transducers for the specific task of making bottom- scattering measurements.

This report will discuss the performance requirements and details of the design development process that resulted in a single transducer that demonstrates very good agreement between performance and theoretical expectations.

PERFORMANCE REQUIREMENTS

The character of the measurements made in the NAVOCEANO project required an acoustic projector with the following general specifications:

- An omnidirectional transducer capable of radiating at 25 kHz, a minimum sound-pressure level (SPL) of 195 dB re 1 μPa at 1 m with an applied voltage of 500 V rms, and capable of operating over the wide frequency band between 5 and 50 kHz.
- Capability of withstanding hydrostatic pressure to 7 MPa (700-m depth).
- A pressure housing large enough to accept a transformer or inductor to tune the transducer if needed.
- Easy accessibility to the pressure housing to allow changes as necessary and be fitted with environmental connectors suitable for use at 7 MPa.
- Rugged enough to withstand rough handling aboard ship or in accidental contact with the ocean floor.

The measurement also required a detection capability with the following general specifications:

- A low-noise preamplifier capable of driving 700 m of cable.
- Low self-noise.
- Stable preamplifier gain of 20 dB at 25 kHz.
- At least 60 dB of dynamic range.
- Low-frequency roll-off at 5 kHz (-3 dB down).
- Circuit damage protection from high-power-supply voltages and high-level transient voltages.
- Maximum recovery time after transient overload to be less than 100 ms.
- Low output impedance, typically 50 Ω.

ACOUSTIC ANALYSIS

The obvious choice for an omnidirectional radiator is a spherical source that, because of its symmetry, radiates sound uniformly in all directions. Since a relatively high SPL was required from the transducer at 25 kHz, the radiator was designed to be resonant near that frequency. The resonance frequency f_r of a spherical ceramic element is given by Mason [1] as

$$f_r = \frac{1}{2\pi a_m \sqrt{\rho_c S_c^E}} , \qquad (1)$$

where a_m is the mean radius, ρ_c is the density of the ceramic, $S_c^E = 1/2\ (S_{11}^{E^m} + S_{12}^E)$ is the mechanical compliance at constant electric field for the radial mode, and S_{11}^E and S_{12}^E are elastic compliance constants. By solving Eq. (1) for a_m and substituting the parameters for Type I ceramic [2] (chosen for stability under high electrical drive), one can determine the radius of the sphere to be about 3.5 cm for a resonant frequency between 25 and 26 kHz. To verify the choice of the element and take into account acoustic loading, however, it was necessary to do a more detailed analysis.

Analysis of the design was accomplished by considering 1) an equivalent circuit that represents a thin-wall ceramic sphere vibrating radially without load, and 2) the circuit for a water-loaded sphere. The response of the water-loaded element was calculated, and the predictions were compared with measured data from the transducer. The analysis is in the form of equivalent circuits based on the voltage-force analogy.

The lumped-constant equivalent circuit for a thin-walled ceramic sphere vibrating radially without load is given in references 1 and 3 and is shown in Fig. 1.

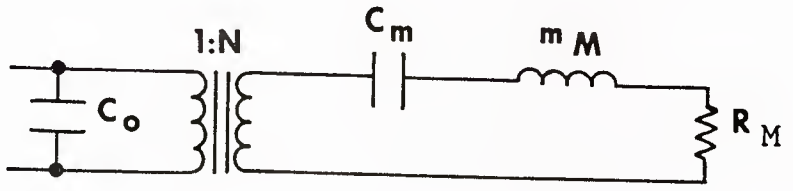

Fig. 1 - Lumped-constant equivalent circuit for a thin-walled ceramic sphere vibrating radially without load.

Removing the transformer in the circuit of Fig. 1 results in the circuit shown in Fig. 2.

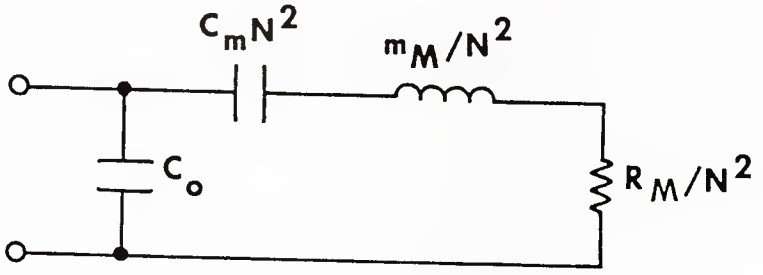

Fig. 2 - Transformed (the results of removing the transformer from Fig. 1) lumped-constant equivalent circuit for a thin-walled ceramic sphere vibrating radially without load.

The values for the components shown in Fig. 2 are computed from the following relations:

Clamped electrical capacitance, $$C_o = 4\pi a_m^2 K_{33}^T \epsilon_0 \frac{1-k_p^2}{t}, \qquad (2)$$

Electromechanical transformer ratio, $$N = \frac{4\pi a_m d_{31}}{S_c^E}, \qquad (3)$$

Mechanical compliance, $$C_m = \frac{S_c^E}{4\pi t}, \qquad (4)$$

Equivalent mechanical mass,

$$m_M = 4\pi a_m^2 t\rho \ , \tag{5}$$

Material mechanical losses,

$$R_M = \frac{a_m\left(\rho\ S_c^E\right)^{1/2}}{C_m Q_m} \ . \tag{6}$$

Each parameter in the equations is identified and has a value given in Table 1 (except the permeability of free space ϵ_0, 8.85×10^{-12} F/m). Table 1 gives the actual physical dimensions and the electromechanical parameters of the sphere used for the radiator; the dimensions were based on the mean radius required by Eq. (1) to provide the desired resonance.

Table 1. Physical parameters and physical constants for G64 piezoelectric ceramic sphere, Type I material

Constant	Parameters
Ceramic mass	0.5 kg
Outside radius a_o	3.72×10^{-2} m
Inside radius a_i	3.28×10^{-2} m
Mean radius a_m	3.5×10^{-2} m
Wall thickness t	4.4×10^{-3} m
Density ρ_o	7.5×10^{3} kg/m^3
Free relative dielectric constant K_3^T	1300
Loss tangent tan δ	0.004
Coupling factor k_p	-0.58
Piezoelectric charge constant d_{31}	-123×10^{-12} C/N
Mechanical quality factor Q_m	500
Piezoelectric voltage constant g_{33}	26.1×10^{-3} Vm/N
Piezoelectric voltage constant g_{31}	-11.1×10^{-3} Vm/N
Elastic compliance constant S_{11}^E	12.3×10^{-12} m^2/N
Elastic compliance constant S_{12}^E	-4.05×10^{-12} m^2/N
Mechanical compliance constant S_C^E	4.124×10^{-12} m^2/N

Table 2 shows the values for the circuit elements computed from Eqs. (2) through (6) and shown in Fig. 2.

Table 2. Computed values of the circuit elements

Elements		Values
C_o	=	27.3×10^{-9} F
N	=	13.12
C_m	=	7.634×10^{-11} m/N
m_M	=	0.5 kg
R_M	=	159.3 N sec/m

The components for the radiation load were derived and added to the circuit of Fig. 2 to represent the loaded sphere as follows. The radiation impedance Z_R for a spherical source radiating into an unbounded medium is given as [4]

$$Z_R = \rho_0 c_0 S_0 \left[\frac{jka_0}{1+jka_0}\right] , \tag{7}$$

where c_0 is the speed of sound in water, ρ_0 is the density of water, S_0 is the surface area of the radiating sphere of radius a_0, and $k = 2\pi f/c_0$ where f is the frequency. The real part of the radiation impedance is

$$R_R = \rho_0 c_0 S_0 \left[\frac{(ka_0)^2}{1+(ka_0)^2}\right] , \tag{8}$$

and the reactive part is

$$X_R = \rho_0 c_0 S_0 \left[\frac{jka_0}{1+(ka_0)^2}\right] . \tag{9}$$

It should be noted that the sphere under consideration is relatively well loaded--that is, the radiation impedance of the sphere almost matches the characteristic impedance of the medium. The value of ka is 3.9 at 25 kHz, and the real part of the radiation impedance is almost 4 times greater than the imaginary. Therefore the imaginary part of the impedance will contribute less than 5% to the total magnitude of the radiation impedance; as a result, the resonant frequency in water is lowered very little by the water load. For ka = 3.9, the equivalent series reactance is $\omega M_R = 0.25\ \rho_o c_o S_o$ where M_R is the added mass due to the water load. For the given sphere, $M_R = 0.04$ kg as compared to 0.5 kg for the ceramic. Also, the ratio of the air-loaded resonance frequency to the water-loaded resonance frequency is

$$\frac{fa}{f\omega} = \sqrt{\frac{0.5}{0.5+0.04}} \qquad (10)$$

or -3.8%. Thus, the unloaded resonance frequency will be virtually the same as the loaded.

The radiation impedance was added to the equivalent circuit of the free sphere as a parallel resistance and inductance, as is done in Fig. 3. The resistive part is $R_R = S_0 \rho_0 c_0$, and the reactive part X_R is exactly represented by the equivalent inductance $M_R\omega$ where $M_R = S_0 \rho_0 a_0$ (see Appendix) is the acoustic mass. The nodes in Fig. 3 are numbered to conform to the requirements of the computer network analysis program used to evaluate the circuit. Since the transducer was to be used with a 374-m electromechanical cable, a capacitance C_c (equal to 36 nF) was added to the equivalent circuit shown in Fig. 3 between nodes 0 and 1 to simulate the cable.

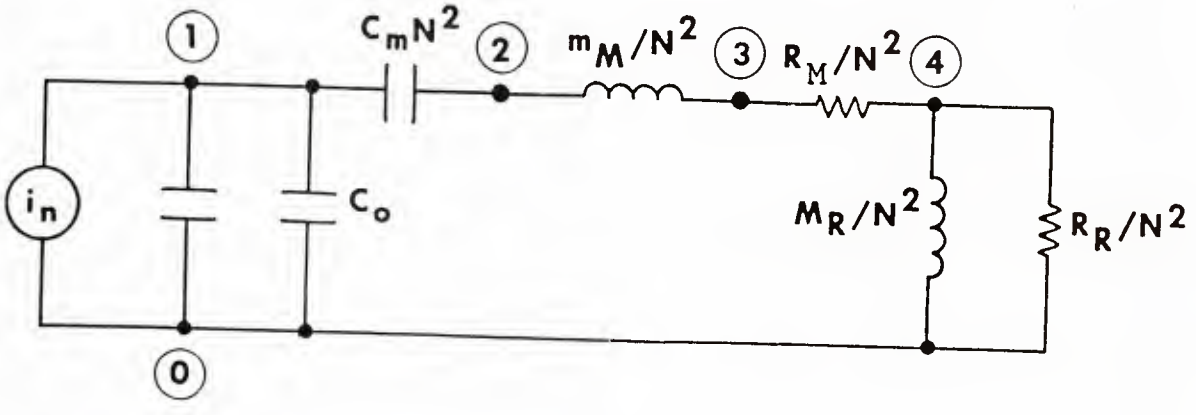

Fig. 3 - Transformed equivalent circuit for a thin-walled ceramic sphere vibrating radially with radiation load, and with a constant current generator. (Nodes numbered to correspond to ac analysis computer program.)

A constant current generator has been added at the input of the circuit to derive the transmitting current response (TCR) for the radiator. If an input current of 1 A is specified, the power dissipated across R_R will be equal to the acoustic power P_a produced when the directivity factor is unity as for an omnidirectional source. Therefore, the TCR in decibels re 1μPa/A at 1 m is

$$TCR = 10 \log P_R + 170.8 \text{ dB}, \tag{11}$$

where P_R is the power dissipated in R_R and 170.8 dB is the sound pressure in μPa at a distance of 1 m from an omnidirectional source referenced to an acoustic power of 1 W.

The theoretical transmitting voltage response (TVR) was determined from the TCR and the input impedance of the circuit where

$$TVR = TCR - 20 \log Z \text{ (dB)}. \tag{12}$$

Since the principle of reciprocity prevails, the reciprocity parameter was used to determine the theoretical free-field voltage sensitivity (FFVS) of the circuit

$$FFVS = TCR - (J), \tag{13}$$

where J is the reciprocity parameter in $VA/\mu Pa^2$. This result is the sensitivity of the transducer at the end of the electromechanical cable without a preamplifier.

THEORETICAL AND MEASURED PERFORMANCE

The equivalent circuit of Fig. 3 was used to predict the performance of the transducer. The theoretical TVR is shown in Fig. 4. Analysis of the equivalent circuit predicted a TVR at 25 kHz of 148 dB re 1μPa/V at 1 m.

Figure 4 also shows the measured TVR for the transducer equipped with a 374-m electromechanical cable; there is good agreement between the predicted and measured responses at frequencies to about 25 kHz. The agreement above 25 kHz becomes poor; in fact, the measured TVR is much larger than the theoretical. This is because the large housing of the transducer causes the response to become directional where omnidirectionality has been assumed in the analysis. In addition, about an octave above resonance, the assumptions of a lumped-parameter model are no longer valid and a distributed parameter analysis must be used.

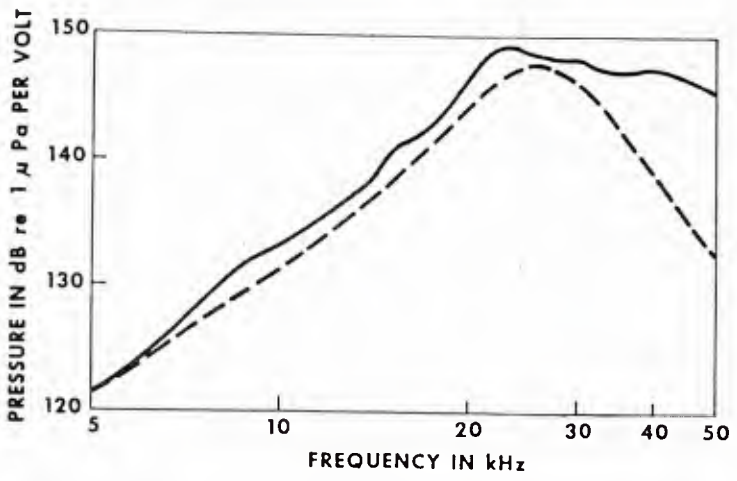

Fig. 4 - TVR of bottom-scattering transducer.
----- Theoretical TVR predicted by the circuit of Fig. 3.
——— Measured TVR for the transducer equipped with a 374-m cable.

The design objective was a minimum SPL at 25 kHz of 195 dB with the application of 500 V (54 dBV). The SPL would be 202 dB with 500 V, which is more than twice the SPL required by the specifications. The wall thickness of the ceramic used for the transducer is 0.44 cm. Based on an average maximum cw drive level of 200 V/mm for Type I ceramic, the transducer can be driven with voltages up to 860 V rms if required. However, only 200 V (46 dBV) was required at 25 kHz to produce an SPL of 195 dB. The efficiency of the transducer at 25 kHz when omnidirectionality is assumed is given by

$$\eta\text{dB} = \text{TCR} - 10 \log R_S - 170.8, \tag{14}$$

where R_S is the equivalent series resistance measured at the input terminals of the transducer--in this case, 70 Ω. This gives

$$\eta\text{dB} = 189 - 18.5 - 170.8 = -0.3 \text{ dB}, \tag{15}$$

or about 97% efficient.

Figure 5 shows the theoretical current response derived by analysis of the circuit shown in Fig. 3 along with the TCR measured in the USRD Lake Facility. The transducer was equipped with the 374-m electromechanical cable.

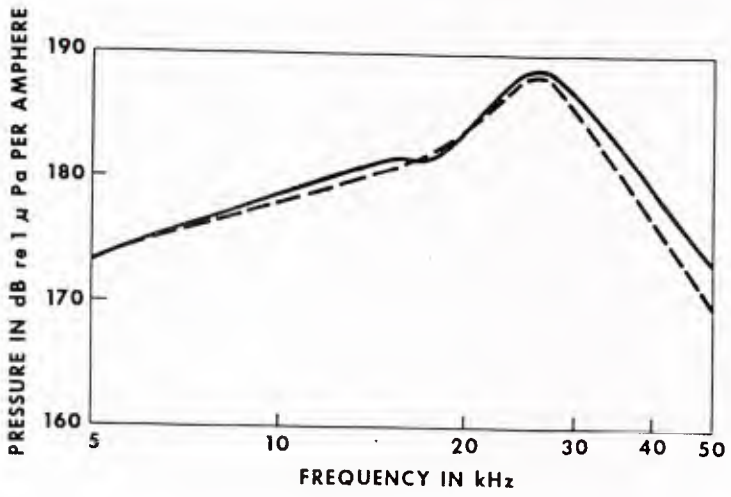

Fig. 5 - TCR of bottom-scattering transducer.
----- Theoretical TCR predicted by the circuit of Fig. 3
——— Measured TCR for the transducer equipped with a 374-m cable.

From the J parameter and the theoretical TCR, the theoretical FFVS at the end of a 374-m electromechanical cable was derived for the transducer. The predicted FFVS is shown in Fig. 6 along with the measured FFVS. The measured FFVS indicated an undulation in the response between 15 and 20 kHz. The same effect is also indicated in the measured TCR and TVR but is not nearly so obvious. This spurious resonance is also attributable to the transducer housing.

Comparison of the theoretical and measured performances shows that the transducer is more than adequate for its intended purpose as a projector. In practice, the transducer was easy to drive and no inductor was needed for tuning.

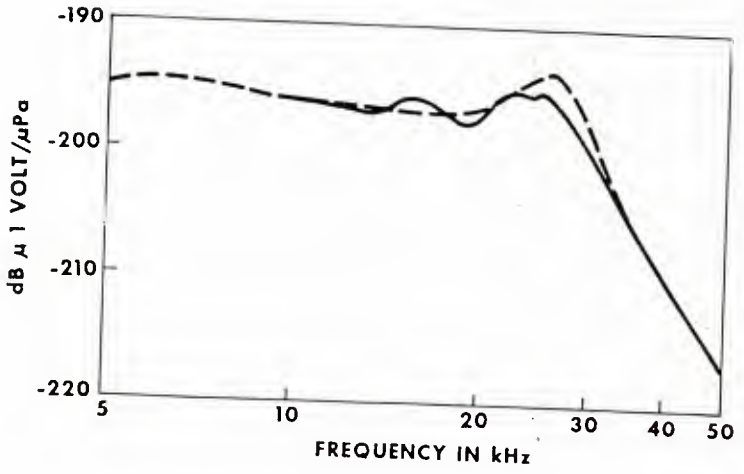

Fig. 6 - FFVS of bottom-scattering transducer
----- Theoretical FFVS at the end of a 374-m cable
——— FFVS measured in the USRD Lake Facility.

A requirement for the transducer was omnidirectional response at frequencies to 25 kHz. The directional response for the transducer is shown in Figs. 7a and 7b. Figure 7a indicates the typical directivity in the XY plane (horizontal) at frequencies to 30 kHz, while 7b indicates the XZ plane (vertical). At frequencies below about 10 kHz, the transducer is virtually omnidirectional but, of course, the preamplifier-transformer housing (described later) perturbs the directivity in the XZ plane at higher frequencies. The specifications for a large housing and for omnidirectionality are in conflict; therefore the design represents a compromise.

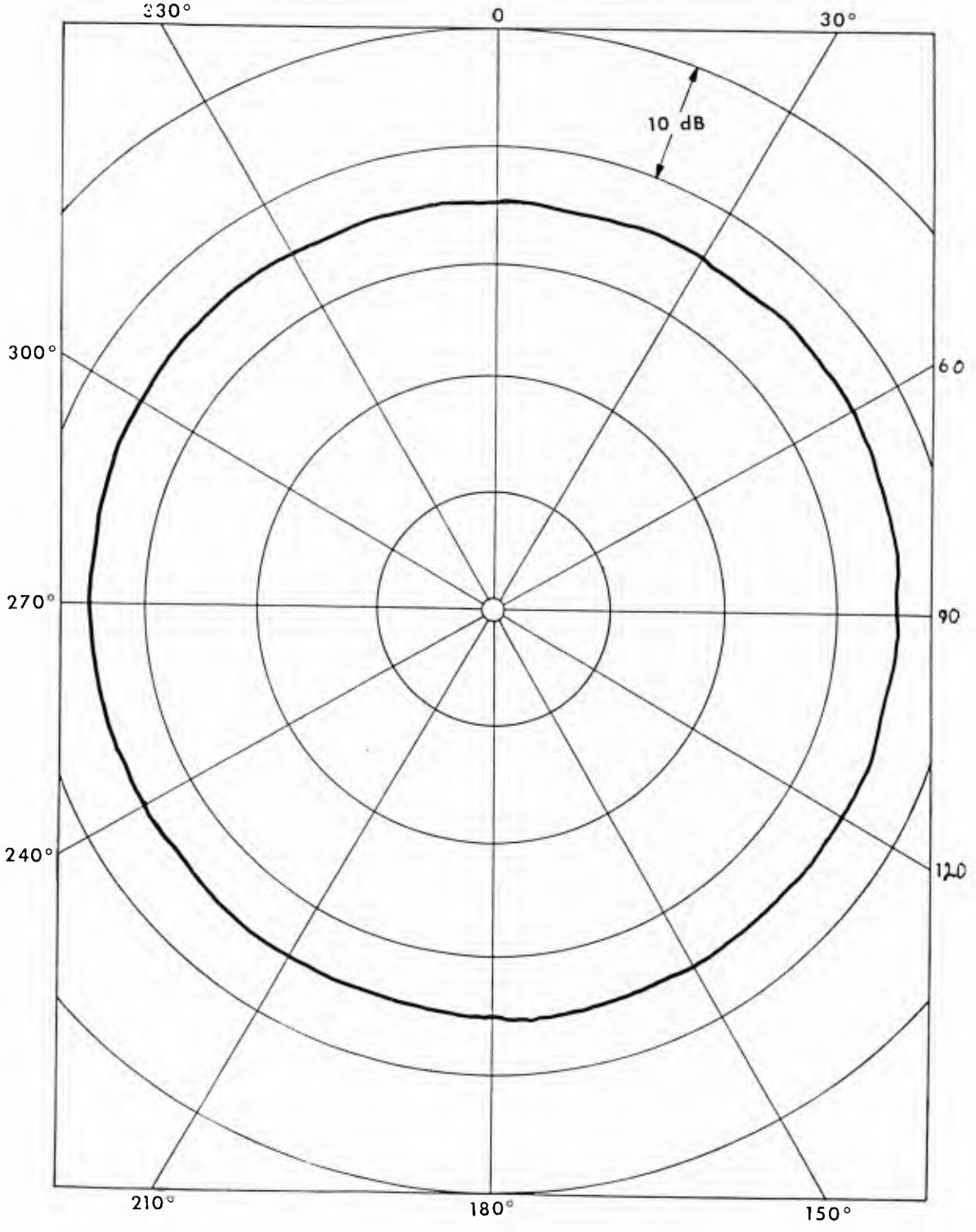

Fig. 7a - Typical directivity of bottom-scattering transducer in the XY plane at frequencies to 30 kHz.

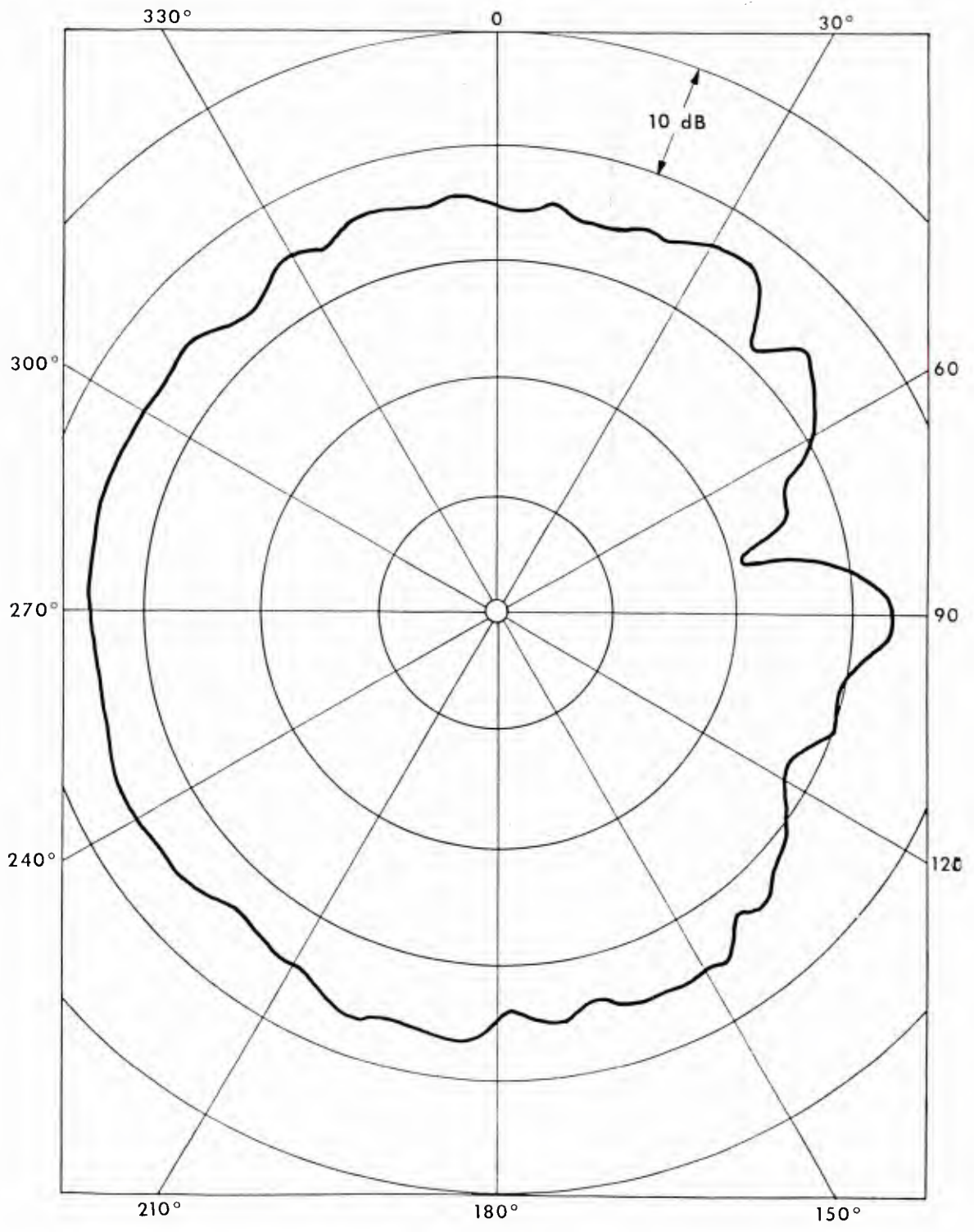

Fig. 7b - Typical directivity of bottom-scattering transducer in the XZ plane at frequencies to 30 kHz.

PREAMPLIFIER DESIGN

It was specified that the transducer be fitted with a low-noise preamplifier to allow it to be used as a conventional hydrophone when desired. The bandwidth specification for the preamplifier indicates that a conventional low-noise operational amplifier was ideally suited for the preamplifier design. Since the frequency range of interest is above 5 kHz, the input stage need not be a field-effect transistor, as is usually the case in hydrophone preamplifiers. An operational amplifier was chosen for the input because the impedance of the sensor is low, with the worst case being about 700 Ω at 5 kHz. The preamplifier is, therefore, a straight-forward op-amp design accomplished with readily available components.

A schematic diagram of the preamplifier is shown in Fig. 8.

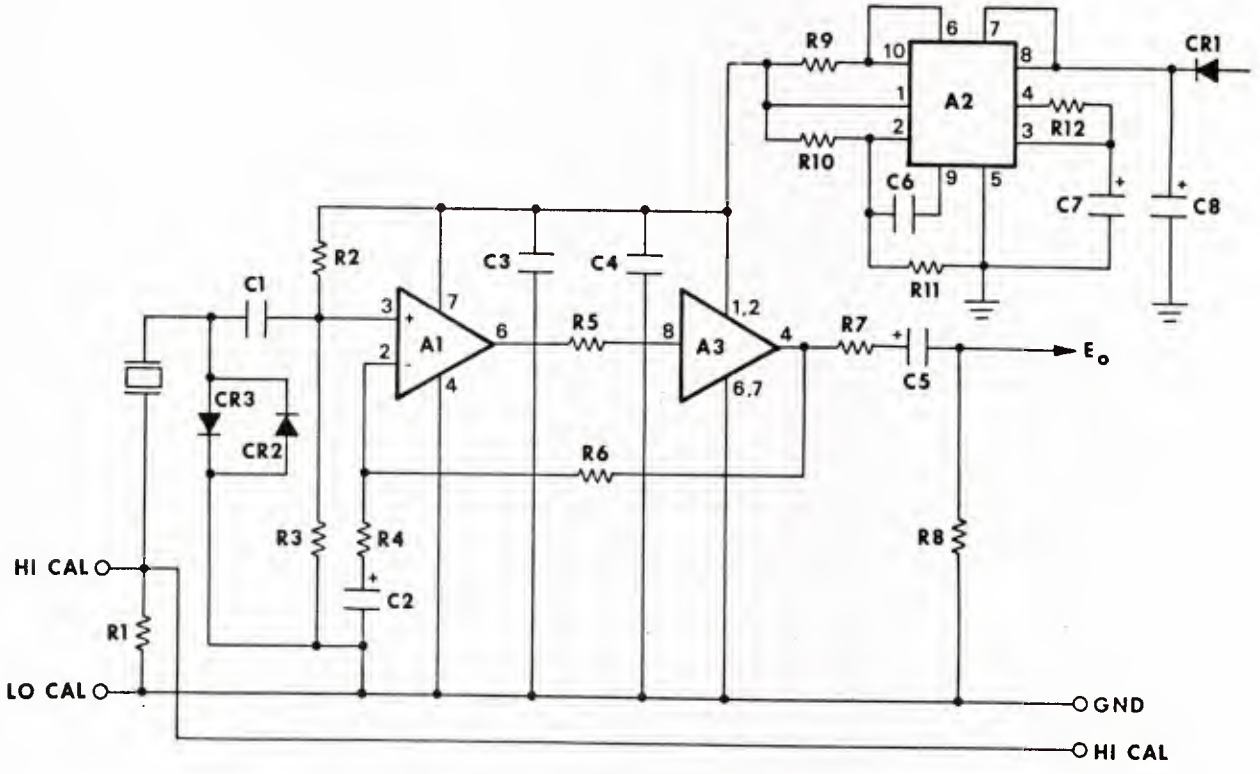

Fig. 8 - Schematic diagram of bottom-scattering transducer preamplifier.

The values for the components shown in Fig. 8 are given in Table 3. The preamplifier is an integration of operational amplifier A1 and current amplifier A3 in a closed-loop configuration to increase output current and maintain linearity when high output signals demand high ac currents from A3. Operational amplifier A1 is a low-noise amplifier used in a non-inverting configuration. It is internally compensated for gains equal to or greater than 3. Power for the preamplifier is supplied to the input of

voltage regulator A2. The output of A2 provides regulated dc power to A1 and A3.

Table 3. Component values for preamplifier circuit

Component	Value	Type
A1	SE5534AH	Signetics
A2	μ723	Fairchild
A3	LH0002 H	National
CR 3 & 4	2N929 Base Collector Junctions	National
R1	10 Ω	RN 60
R2 & 3	40K	RN 55
R4	2K	RN 55
R5	100 Ω	RN 55
R6	18K	RN 55
R7	37.5 Ω	RN 55
R8	100K	RN 55
R9	10 Ω	RN 55
R10	1.5K	RN 55
R11	1K	RN 55
R12	619 Ω	RN 55
C1	0.1 μF	CK05BX
C2	0.015 μF	MIL-39003
C3 & C4	0.01 μF	CK05
C5	56 μF 50V	MIL-39003
C6	1 μF 50V	MIL-39003
C7	100 pF 200V	CK05
C8	4.7 μF	MIL-39003
CR5	1N4001	Motorola

If one refers to the input of the preamplifier as shown in Fig. 8, the sensor element is ac coupled to the input of A1 by coupling capacitor C1. The input of A1 is internally protected by diodes, but external diodes CR3 and CR4 have been added for redundant protection against voltage transients. Laboratory measurements and acoustic measurements have shown that the preamplifier will recover from a several volt overload in about 60 μs, which is well within the design requirements. Diodes CR3 and CR4 limit the input level to about 0.5-V peak. The diodes rapidly go into conduction at higher voltage and limit the input level. The diodes also protect the circuit input against a buildup of dc potential across CY as well as transients. One should note that CR3 and CR4 have a dynamic resistance long before they go into full conduction. The value of resistance changes as a function of bias or input level; and in cases where the sensor impedance is very high, the low-frequency roll-off will vary as a function of input level. In the present case, however, the

diodes are more than adequate because the sensor impedance is low, the preamplifier input impedance is low, and the low-frequency roll-off is high (see Fig. 9).

Operational amplifier A1 was chosen for the input device because of its low self noise; the typical noise voltage at 1 kHz is 4 nV/$\sqrt{\text{Hz}}$ or -168 dB re 1 V/Hz. Obviously, other characteristics such as open-loop gain and slew rate are important, but both of these characteristics are more than adequate for this application.

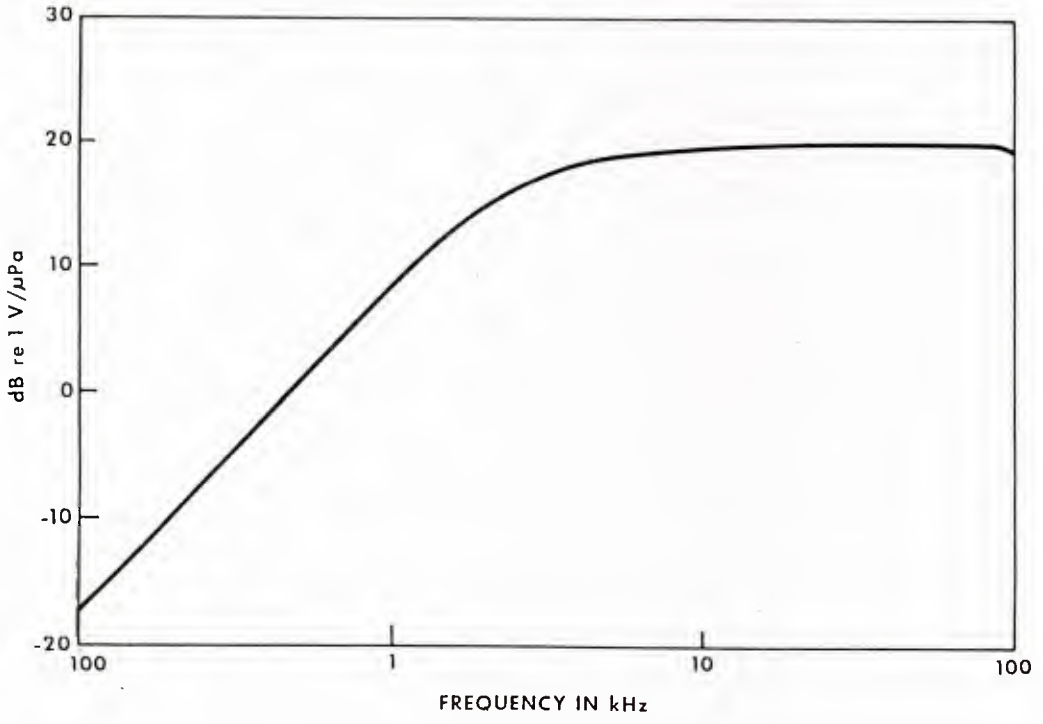

Fig. 9 - Gain transfer function for preamplifier.

Resistor R2 and R3, which are equal in value, establish the ac operating points for A1 and A2 between the dc supply voltage and ground. The resistors in conjunction with the sensor capacitance CY form a single-pole high-pass filter. The break frequency is

$$f_{-3dB} = \frac{1}{2\pi\left(\frac{R2 \times R3}{R2+R3}\right)CY}, \qquad (14)$$

or about 170 Hz.

Line driver A3 is an integrated-circuit, unity-gain current amplifier. Its ideal characteristics are high input impedance and low output impedance, typically 400 kΩ and 12 Ω, respectively. The output of A3 is configured by resistor R7 to match the output impedance to a 50-Ω coaxial cable or for termination to minimize line reflections. In actual use, the hydrophone cable was not terminated because there was no problem with standing waves. However, this feature was incorporated into the design to be available if needed. Though oscillation is not a problem with this design, a damping resistor R5 has been placed at the input of A3 to ensure oscillation suppression.

The gain of the preamplifier A is set by resistors R4 and R6 where

$$A_v(\text{dB}) = 20\log(1+R6/R4) = 20 \text{ dB} . \qquad (15)$$

As previously noted, line-driven A3 is included in the feedback loop of A1 but its presence has no effect on the circuit gain since it is an ideal current source.

A single-pole, high-pass filter is formed by R4 and the ac by-pass capacitor C2, which results in a break frequency of 5.3 kHz. This is slightly higher than the requested 5 kHz but consistent with standard component values.

Voltage regulator A2 provides 18-Vdc regulated power to A1 and A3. The input to A2 is filtered by capacitor C6 and is reverse-voltage protected by diode CR5. A small bypass capacitor C3 and C4 is placed at the V+ terminal of A1 and A3 to cancel power-supply lead inductance--a conservative step to further suppress possible oscillations.

A summary of the characteristics of the preamplifier is given in Table 4. Figure 9 shows the gain transfer characteristics of the preamplifier as a function of frequency with a 47,000-pF capacitor simulating the free capacitance of the sensor element. Figure 10 indicates the FFVS measured at the end of a 374-m electromechanical cable for the transducer equipped with the preamplifier.

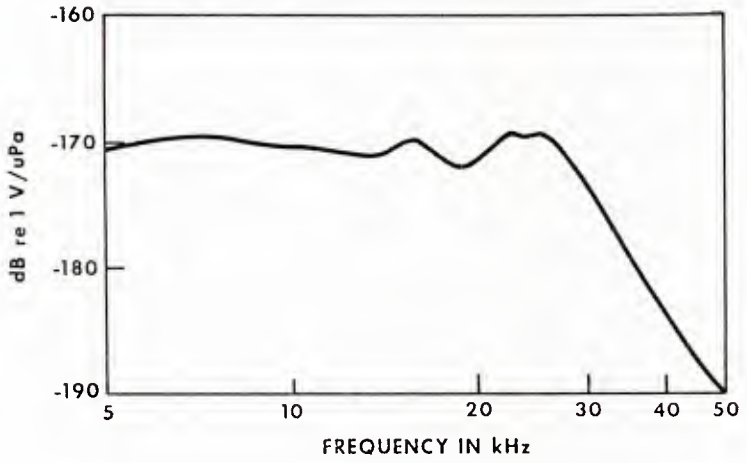

Fig. 10 - FFVS of bottom-scattering transducer used as a hydrophone with the described preamplifier.

Table 4. Preamplifier Characteristics

Power Supply Voltage	24 Vdc
Quiescent Supply Current	19.2 ma
Gain	20 dBV
Bandwidth	5 to 100 kHz
Input Impedance	20 kΩ
Output Impedance	50 Ω
Maximum Input Voltage for 1% THD Measured at Output	380 mVΩ
Self Noise 5 to 30 kHz measured at the output and referred to the input with a 47,000-pF load on the input	7 nV/vHz (-163 dBV)
Overload recovery time	60 μs

TRANSDUCER DESIGN

The transducer/hydrophone developed for NAVOCEANO has been designated the USRD type G64 transducer.

Details of the construction of the G64 are shown in a sectional view in Fig. 11 and in a photograph in Fig. 12.

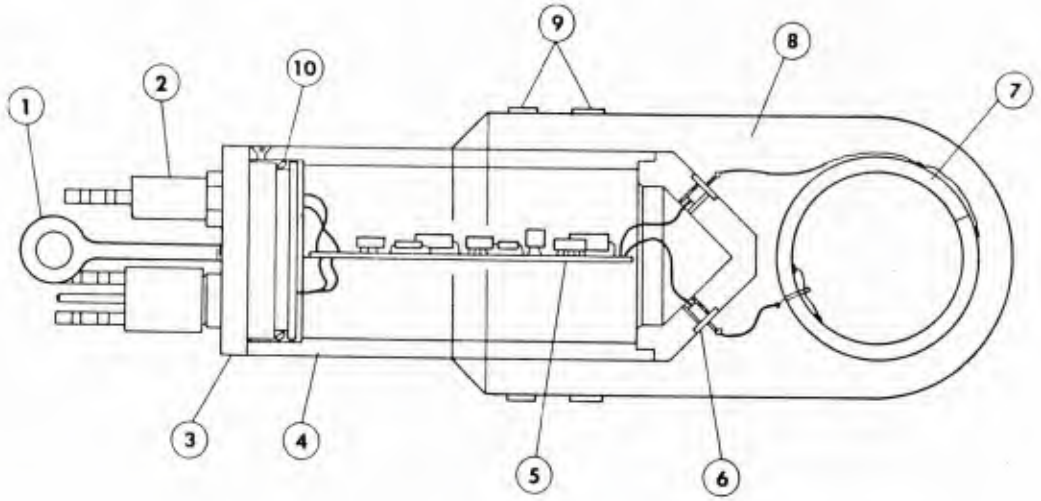

Fig. 11 - Sectional view of bottom-scattering transducer, USRD type G84, showing:

1 - stainless-steel eyebolts	6 - hermetic seals
2 - Electro connector	7 - Type I ceramic sphere
3 - access port	8 - PRC 1538 polyurethane
4 - stainless-steel housing	9 - stainless-steel bonding
5 - preamplifier-transformer	10 - O-ring

The active element is a 7.4-cm-diam, 4.3-mm-wall Type I ceramic sphere. The acoustic window for the ceramic element is formed by encapsulating the sensor in PRC 1538 black polyurethane. The polyurethane is bonded to the stainless-steel housing and ceramic element in one potting operation. The sectional area of the potting is thick to protect the sensor from shipboard mishandling or damage from contact with the ocean bottom when in service. Stainless-steel bands clamp the polyurethane to the housing to reduce the effects of bond failure should it occur. The housing, suspension eyebolts, and other metal parts exposed to seawater are made of Type 316 stainless steel. The bulkhead with eyebolts and electrical connector is easily removed to allow access to the preamplifier-transformer area of the housing. The bulkhead is sealed by an O-ring and secured by stainless-steel, flat-head machine screws. Transducer drive and/or hydrophone signal output and input power are provided via a 4-contact Electro Series 53 connector. Hydrophone coupling measurements can be made by a signal input on a 2-contact Electro connector.

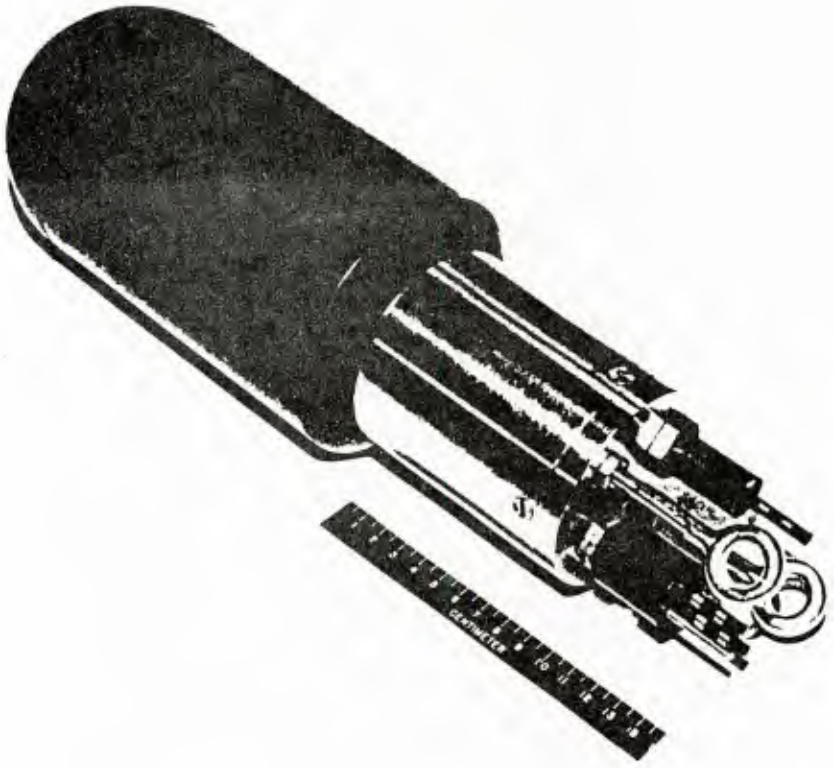

Fig. 12 - Photograph of USRD type G64 transducer

SUMMARY

A transducer has been designed and developed for use in ocean-bottom-scattering measurements by NAVOCEANO. The requirements for the design have been presented, mathematical modeling and analysis of the design have been performed, and data have been given to compare the theoretical results with the measured results. The design of a low-noise preamplifier made with integrated circuits to complement the transducer and allow it to be used as a hydrophone has been presented. The USRD type G64 transducer has been accepted and used with good results by NAVOCEANO to fulfill their mission requirements.

REFERENCES

1. Warren P. Mason, Physical Acoustics (Academic Press, New York, 1964) Vol. 1 Part A, p 224.

2. "Military Standard Piezoelectric Ceramics for Sonar Transducers", DOD STD-1376A(SH) (GPO, Washington, DC, 1970).

3. T.A. Henriquez, "The USRD Type F39A 1-kHz Underwater Helmholtz Resonator", NRL Report 7740, 10 April 1974.

4. L.L. Beranek, Acoustics, (McGraw-Hill Inc., New York, 1954) p 36.

APPENDIX - Derivation of the Specific Acoustic Impedance

The specific acoustic impedance of a spherical source radiating radially is given in Reference 3 as

$$Z = \rho_0 c_0 \left[\frac{(ka_0)^2}{1+(ka_0)^2} + j \frac{ka_0}{1+(ka_0)^2} \right] . \tag{A1}$$

The mechanical impedance Z_m is simply $Z_m = S_0 Z$, where S_0 is the area of the spherical source

$$S_0 = 4\pi a^2 \tag{A2}$$

and a is the outside radius.

The impedance can be exactly represented as a parallel combination of a radiation resistance

$$R = S_0 \rho_0 c_0 \tag{A3}$$

and a radiation mass

$$M = S_0 \rho_0 a_0 , \tag{A4}$$

as shown in Fig. A1.

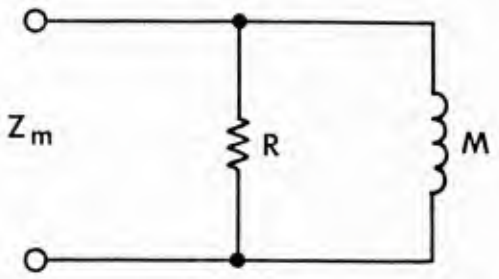

Fig. A1 - Equivalent circuit of mechanical impedance Z_m.

The classical solution for Z_m, as shown in Fig. A1, has the form

$$Z_m = \frac{j\omega RM}{R+j\omega M} \cdot \tag{A5}$$

Multiplying the numerator and denominator of Eq. (A5) by j and -1 gives

$$Z_m = \frac{\omega RM}{\omega M - jR} \cdot \tag{A6}$$

Taking the complex conjugate of Eq. (A6) and substituting for R, M, and ω where $\omega = kc$ gives

$$Z_m = \frac{\omega S_0^{\,3} \rho_0^{\,3} c_0 a_0 (\omega a_0 + jC)}{S_0^{\,2} \rho^2 \left[(\omega a_0)^2 + c^2\right]} = S_0 \rho_0 c_0 \left[\frac{(ka_0)^2}{1+(ka_0)^2} + j\,\frac{ka_0}{1+(ka_0)^2}\right], \tag{A7}$$

which is the same as ZS_0 in Eq. (A1).

Superintendent
Naval Postgraduate School
Attn: Technical Library
Monterey, CA 93943